Uncertainty Analysis for Noise-Parameter Measurements at NIST

James Randa, *Senior Member, IEEE*

***Abstract*—An uncertainty analysis is presented for the National Institute of Standards and Technology (NIST) measurements of the noise parameters of amplifiers and transistors in both connectorized (coaxial) and on-wafer environments. We treat both the X-parameters, which are based on the wave representation of the noise correlation matrix, and the traditional IEEE noise parameters. The type A uncertainties are obtained from the fit that computes the noise parameters from an overdetermined system of equations, and the type B uncertainties are computed by a Monte Carlo program. Some complications that are explicitly discussed include the effect of an output attenuator or probe, physical bounds, and the occurrence of unphysical results. Some sample results are given.**

***Index Terms*—Amplifier noise, measurement uncertainty, Monte Carlo (MC), noise figure, noise measurement, noise parameters, transistor noise, uncertainty.**

I. Introduction

The National Institute of Standards and Technology (NIST) has recently modified and expanded its noise-parameter measurement methods and analysis for amplifiers and on-wafer transistors [1], [2]. For the measurements to be meaningful, the results must be accompanied by their corresponding uncertainties. This paper describes the procedures that are used to estimate the standard uncertainties in NIST's measurements of noise parameters. An abbreviated summary was presented at the 2008 Conference on Precision Electromagnetic Measurements (CPEM 2008) [3], and the full details can be found in [4].

The noise parameters are computed by performing a least-square fit to an overdetermined system of equations, which is obtained by measuring the output noise temperature (or power) for each of a number of different input terminations connected to the amplifier or transistor under test. The type A uncertainties can be computed from the covariance matrix of the fitted parameters, but the type B uncertainties require more effort. The uncertainties in the underlying or input quantities, such as reflection coefficients, measured noise temperatures, etc., are known or can be estimated, but the problem of propagating these underlying uncertainties to compute the uncertainties in the output noise parameters does not admit a simple analytical solution. Therefore, a Monte Carlo (MC) approach is used for the type B uncertainties. Matters are further complicated by the fact that it is convenient to perform our analysis in terms of one set of noise parameters (what we call the X-parameters), but we need to express our results and uncertainties in terms of a different set (the IEEE noise parameters) that is in near-universal use.

In Section II, we review the measurement and analysis method as well as the MC technique. Only very brief summaries are given since these topics have been covered elsewhere [1], [2], [5] or (as in the case of the MC technique) are in widespread use. We instead choose to devote most of our attention to the features of the MC program that are new or unique to the present application. In Section III, we present the uncertainties used for the quantities that are measured directly. The special difficulties that arise for large output reflection coefficients are treated in Section IV. Section V discusses the physical bounds on the noise parameters and the enforcement of these bounds in the MC program. Some sample results and conclusions are presented in Section VI.

II. Framework

A. Measurement and Analysis

Our theoretical framework was set out in [5], following the representation of Wedge and Rutledge [6]. The 2×2 noise correlation matrix of a two-port device in the wave representation is defined by

$$N_{i,j} \equiv \left\langle c_i c_j^* \right\rangle \tag{1}$$

where c_1 and c_2 are the (complex) amplitudes of the waves emerging from the input and output ports of the device due to its intrinsic noise, and the brackets indicate an average over time or ensemble (assumed to be equal). The normalization of the wave amplitudes is such that their magnitudes squared are spectral power densities. For convenience, we define and work with temperature variables that correspond to scaled elements of the noise correlation matrix

$$\begin{aligned} k_B X_1 &\equiv \left\langle |c_1|^2 \right\rangle \\ k_B X_2 &\equiv \left\langle |c_2/S_{21}|^2 \right\rangle \\ k_B X_{12} &\equiv \left\langle c_1 (c_2/S_{21})^* \right\rangle \end{aligned} \tag{2}$$

where k_B is Boltzmann's constant, and where dividing each c_2 by S_{21} effectively refers all four noise parameters (X_1, X_2, ReX_{12}, and ImX_{12}) to the input plane 1.

Manuscript received June 10, 2008; revised September 15, 2008. First published November 25, 2008; current version published March 10, 2009. This work was supported in part by Agilent Corporation. The Associate Editor coordinating the review process for this paper was Dr. Tae-Weon Kang.

The author is with the Electromagnetics Division, National Institute of Standards and Technology, Boulder, CO 80305 USA, and also with the Physics Department, University of Colorado at Boulder, Boulder, CO 80309 USA (e-mail: randa@boulder.nist.gov).

Digital Object Identifier 10.1109/TIM.2008.2007044

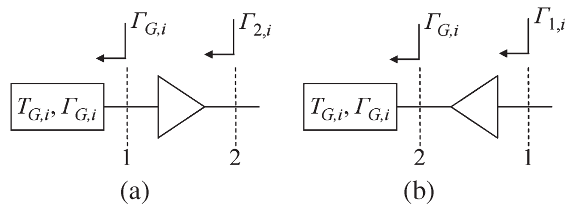

Fig. 1. (a) Forward and (b) reverse measurement configurations.

The measurement method for either off-wafer ("connectorized") amplifiers or on-wafer transistors (or amplifiers) consists of connecting a series of different known terminations i to one of the ports of the device under test (DUT) and measuring the resulting noise temperature at the other port. The noise parameters are then computed by performing a weighted least-square fit to the equations for the measured noise temperatures as functions of the noise parameters. Most or all of the measurements are performed in the forward configuration of Fig. 1(a), in which the known termination $(\Gamma_{G,i}, T_{G,i})$ is connected to the input port, and the noise temperature $(T_{2,i})$ is measured at the output port. In the case of poorly matched devices, which are typically transistors on a wafer, it is advantageous to also perform at least one reverse measurement, as in Fig. 1(b). In terms of the X-parameters of (2), the output noise temperature at plane 2 in Fig. 1(a) is given by

$$T_{2,i} = \frac{|S_{21}|^2}{(1-|\Gamma_{2,i}|^2)} \left\{ \frac{\left(1-|\Gamma_{1,i}|^2\right)}{|1-\Gamma_{1,i}S_{11}|^2} T_{i,1} + \left| \frac{\Gamma_{1,i}}{1-\Gamma_{1,i}S_{11}} \right|^2 X_1 + X_2 + 2\mathrm{Re}\left[\frac{\Gamma_{1,i}X_{12}}{1-\Gamma_{1,i}S_{11}} \right] \right\} \quad (3)$$

and for the reverse configuration of Fig. 1(b), the equation is

$$T_{1,i} = \frac{1}{(1-|\Gamma_{1,i}|^2)} \left\{ \frac{|S_{12}|^2 \left(1-|\Gamma_{2,i}|^2\right)}{|1-\Gamma_{2,i}S_{22}|^2} T_{2,i} + \left| \frac{S_{12}S_{21}\Gamma_{2,i}}{1-\Gamma_{2,i}S_{22}} \right|^2 X_2 + X_1 + 2\mathrm{Re}\left[\frac{S_{12}S_{21}\Gamma_{2,i}X_{12}^*}{1-\Gamma_{2,i}S_{22}} \right] \right\}. \quad (4)$$

In the NIST noise parameter measurements, the value of $G_0 \equiv |S_{21}|^2$ is also treated as a free parameter and is determined by the fit to the noise measurements.

The most commonly used set of noise parameters is the IEEE set [7]. It is, therefore, desirable to present any measurement result in terms of the IEEE set, in addition to the results for the X's. Even within the IEEE set, there are several variants; we use the set in which the effective input noise temperature T_e is given by

$$T_e = T_{\min} + t \frac{|\Gamma_{\mathrm{opt}} - \Gamma_G|^2}{|1+\Gamma_{\mathrm{opt}}|^2 \left(1-|\Gamma_G|^2\right)} \quad (5)$$

where Γ_G is the reflection coefficient of the input termination at plane 1, and the four noise parameters are $T_{\min}$, t, and the complex Γ_{opt}. The parameter t is related to the noise resistance R_n by $t = 4R_nT_0/Z_0$, where $T_0 = 290$ K, and Z_0 is the reference impedance, commonly taken to be 50 Ω. Assuming that the S-parameters are known, the IEEE noise parameters can be calculated from the X's, and *vice versa*. The equations for the transformations can be obtained from the results in [6] and are given in [4].

B. Type A Uncertainties

The noise parameters are computed by a fit to an overdetermined system of equations, and the fitting program returns the covariance matrix V_{ij} for the fitting parameters. The type A uncertainties are then given by the square roots of the diagonal elements

$$u_A(X_i) = \sqrt{V_{ii}(X)} \quad (6)$$

where X_i represents any of the five fitting parameters (X's and G_0).

Since the parameters that are most commonly used are the IEEE parameters, we also need to evaluate the uncertainties in them. Because the fit is performed in terms of the X parameters, the fitting program does not return values or a covariance matrix for the IEEE parameters. The IEEE parameter values are computed from the X parameters, and the covariance matrix for the IEEE parameters must be computed from the X-parameter covariance matrix by using the Jacobian matrix for the transformation. If we use I_i to represent one of the five IEEE parameters (including G_0), then the type A uncertainties in the IEEE parameters are given by

$$u_A(I_i) = \sqrt{V_{ii}(\mathrm{IEEE})}$$
$$V_{ij}(\mathrm{IEEE}) = \sum_{i',j'=1}^{5} \frac{\partial I_i}{\partial X_{i'}} \frac{\partial I_j}{\partial X_{j'}} V_{i'j'}(X). \quad (7)$$

The calculation of the elements of the Jacobian matrix $(\partial I_i/\partial X_{i'})$ is straightforward but tedious, and the results are lengthy and unenlightening. They can be found in [4].

C. MC Evaluation of Type B Uncertainties

In our noise-parameter measurements, the type B uncertainties arise due to the possible errors in the input parameters, which include the amplifier S-parameters, all the measured reflection coefficients, the temperature of the ambient-temperature terminations, the noise temperature of the non-ambient termination(s), and the measured output noise temperatures. We know or can estimate all these input uncertainties, and we adopt an MC approach to deal with the propagation of the input uncertainties into uncertainties in the noise parameters. A good description of the MC approach can be found in [8]. Our own MC procedure is described in full detail in [4].

Before discussing the special features of our MC program, it is useful to note some general elements. The number of simulated measurement sets N_{sim} is chosen to be large enough so that the computed uncertainties are approximately independent of N_{sim}. A value of $N_{\mathrm{sim}} = 10\,000$ is usually more than sufficient, but for poorly matched transistors, it is occasionally necessary to use larger values. In all cases, we use a large enough value that any further increase in N_{sim} changes the uncertainties by at most 10% of their values. In most cases, the uncertainties are within a few percent of their asymptotic values.

Because the input variables include sets of variables that are all measured in the same manner, correlated errors can and do occur, and the correlations can cause significant effects in the noise parameter uncertainties [5]. We therefore include correlated errors in the simulations. The correlations that we include are among all the measured reflection coefficients and S-parameters, among all the output noise temperatures, and among the temperatures of the ambient-temperature terminations. If there is more than one nonambient input termination, we include correlations between them.

Each set of simulated noise-temperature measurements is analyzed in the same manner as a set of real measurements. We perform a (usually nonlinear) least-square fit to the measurement results and obtain a set of noise parameters (X_1, X_2, X_{12}, G_0). From these and the simulated measurement results for the amplifier's S-parameters, we compute the set of IEEE noise parameters ($T_{\min}$, t, Γ_{opt}, and G_0). This is done for each of the N_{sim} sets of simulated measurements. The average and standard deviation of the measured values for each parameter (X and IEEE) are computed. For the complex quantities X_{12} and Γ_{opt}, the statistics are computed separately for the real and imaginary parts. The uncertainties for $|\Gamma_{\mathrm{opt}}|$ are then computed from those for the real and imaginary parts. The (type B) uncertainty in a single measurement of a parameter is then computed by combining the standard deviation in quadrature with the difference between the average and the true value. This is just the root mean square error (RMSE) of the sample

$$u_B(y) = \mathrm{RMSE}(y) = \sqrt{Var(y) + (\bar{y} - y_{\mathrm{true}})^2} \qquad (8)$$

where y is any of the noise parameters, and $Var(y)$ is the variance of the sample of simulated results for y. The fact that $\bar{y}$ is not equal to the true value y_{true} may be unsettling at first, but such are the vagaries of nonlinear functions.

III. Input Uncertainties: Connectorized Case

The simulations require as input not only the true values of all the parameters but also the standard uncertainties in the parameters that are directly measured, i.e., the amplifier S-parameters, the reflection coefficients of all the terminations, the noise temperatures of all the terminations, the output reflection coefficient $\Gamma_{2,i}$ in Fig. 1(a) (if it is measured), and the output noise temperatures. These input uncertainties (or the parameters that determine the uncertainties) are read into the MC program along with the input data so that they can be changed at any time, but we have a standard set of uncertainties that we currently use.

In treating correlated and uncorrelated errors, we introduce correlated and uncorrelated uncertainties that are defined by the relations

$$\begin{aligned} u(y_i)^2 &= u_{\mathrm{unc}}(y_i)^2 + u_{\mathrm{cor}}(y_i)^2 \\ \rho_{ij} &= \frac{u_{\mathrm{cor}}(y_i) u_{\mathrm{cor}}(y_j)}{u(y_i) u(y_j)} \end{aligned} \qquad (9)$$

where "cor" and "unc" refer to correlated and uncorrelated, and ρ_{ij} is the correlation coefficient for errors in y_i and y_j.

The reflection coefficients $\Gamma_{G,i}$ and $\Gamma_{2,i}$ (if it is measured) are measured on a commercial vector network analyzer (VNA). Since all the reflection coefficients are measured with the same calibration on the same VNA, there is a significant correlation among the errors of the different reflection coefficients. The connector used on the radiometer port is type PC-7, and therefore, we assumed that the packaged amplifier also has PC-7 connectors. (If the amplifier has some other connector that requires use of adapters, the uncertainty analysis is similar in form to the on-wafer case, which is treated below.) The uncertainties in the reflection-coefficient measurements can depend on the magnitude of the reflection coefficient; usually, the uncertainties are larger for larger reflection coefficients. Our program uses one value for small $|\Gamma|$ (less than or equal to 0.5) and another for large $|\Gamma|$ (greater than 0.5). In the program, we work in terms of u_{cor} and u_{unc} [defined in (9)] and then compute u and ρ from them. The values typically used for small $|\Gamma|$ are $u_{\mathrm{cor}} = 0.0025$ and $u_{\mathrm{unc}} = 0.001$, which correspond to $u(\Gamma) \approx 0.002693$ and $\rho \approx 0.8621$. These uncertainties are somewhat larger than the manufacturer's specifications, reflecting our own past experience with such measurements [9]. For large $|\Gamma|$, we use $u_{\mathrm{cor}} = 0.004$ and $u_{\mathrm{unc}} = 0.001$, which correspond to $u(\Gamma) \approx 0.004123$ and $\rho \approx 0.9412$. The uncorrelated part of the uncertainty $u_{\mathrm{unc}} = 0.001$ is primarily due to connector (non)repeatability. The same $u(\Gamma)$ is used for both real and imaginary parts of each reflection coefficient, $u(\mathrm{Re}\Gamma) = u(\mathrm{Im}\Gamma) = u(\Gamma)$. The small S-parameters (i.e., S_{11}, S_{22}, and S_{12}) have their errors treated in the same way as the reflection coefficients, including the correlations. For S_{21}, we use $u(\mathrm{Re}S_{21}) = u(\mathrm{Im}S_{21}) = 0.01$. This value was obtained by an extrapolation of the VNA specifications, which do not extend to S_{21} magnitudes as large as we have encountered. The input uncertainties in S_{21} are not very important because the magnitude of S_{21} is treated as a fitting parameter $G_0 = |S_{21}|^2$.

The ambient temperature in the laboratory is set at 296.15 K and is kept within 0.5 K of this value. We therefore use a rectangular distribution extending from 295.65 to 296.65 K for the ambient-temperature terminations. Because several hours intervene between measurements on the amplifier with different terminations, there is essentially no correlation between the errors in the temperatures of different ambient-temperature terminations.

The uncertainty in the measured output noise temperature(s) depends on a number of details, such as the reflection coefficient of the DUT, the magnitude of the noise temperature being measured, the statistics of the multiple repeat measurements, and the characteristics of the radiometer at the measurement frequency. Rather than performing a full evaluation of the uncertainty for each simulated measurement, we use the following approximate parameterization for the uncertainty in the noise-temperature measurements:

$$u(T_{\mathrm{meas}}) = 0.2K + 0.005(T_{\mathrm{meas}} - T_a) \qquad (10)$$

where T_a is the noise temperature that corresponds to the ambient temperature of 296.15 K. This form is adequate, provided

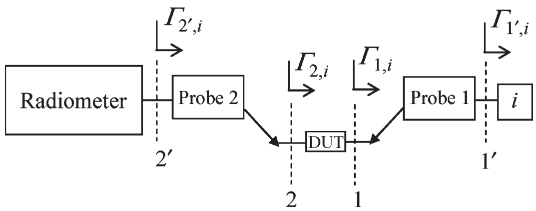

Fig. 2. Reference planes for on-wafer measurements.

that the reflection coefficient of the DUT is less than about 0.2. For larger reflection coefficients, a further refinement is required, as described in Section IV.

There is a significant correlation among the measurements of the output noise temperatures for the different terminations. An examination of the uncertainty analysis that was performed for noise-temperature measurements in coaxial lines [10] leads to the conclusion that most of these errors are typically correlated. The major source of uncorrelated error is the connector (non)repeatability. The magnitude of the connector error relative to the correlated errors would lead to a value $\rho \approx 0.98$. Because the correlated errors in the noise-temperature measurements often lead to much smaller uncertainties [5], we are reluctant to use such a large correlation coefficient without being very sure of it. Until we have better knowledge of these correlations, we will use $\rho = 0.64$, which corresponds to $u_{\rm cor}/u_{\rm unc} = 4/3$. This may lead to a small overestimate of the uncertainty, but we prefer to err on the side of caution.

Further complications, such as the correlation between the measured noise temperature of the nonambient input noise source and the measured output noise temperatures, are dealt with in [4].

IV. Differences for the On-Wafer Case

A. Method and Input Uncertainties

The measurement configuration for an on-wafer amplifier or transistor is shown in Fig. 2 for the forward configuration. The reverse configuration is obtained by turning around the DUT, interchanging planes 1 and 2. The measurement method is similar to that for connectorized amplifiers, except for the differences due to the presence of probes.

To use (3) and (4) between planes 1 and 2, we need the reflection coefficients, S-parameters, and noise temperatures at those planes. The $\Gamma_{G,i}$ in (3) will be $\Gamma_{1,i}$ in Fig. 2. A two-tier calibration is performed using a multiline through-reflect-line (TRL) set of calibration standards [11], [12] that has been fabricated on the wafer. The NIST MultiCal software is used to perform the two-tier calibration. The calibrated VNA is then used to measure the reflection coefficients and transistor S-parameters at planes 1 and 2, as in the amplifier case in the preceding section. The output noise temperatures are measured at plane $2'$ and corrected to plane 2 by treating Probe 2 (and the output attenuator, if present) as an adapter. Similarly, the nonambient input noise temperature at plane 1 is measured with the configuration in Fig. 2 but with the on-wafer device replaced by a through line.

The uncertainty analysis for the measurement of the noise parameters of on-wafer transistors is thus similar to that for measurements on packaged amplifiers, but it presents a few additional complications. Because the measurement planes of interest are on the wafer, we must characterize and correct for the effects of the probes, which introduces additional uncertainty. In addition, the uncertainties in VNA and noise measurements are different on a wafer from what they are in coaxial lines, and therefore, the input uncertainties are different for the on-wafer case. The third complication is that the transistor may be very poorly matched to the connecting transmission lines, leading to relatively large values of the reflection coefficient at its output. This requires that we refine our estimate of the uncertainty in measuring the output noise temperature.

The uncertainty in the noise temperatures of the ambient-temperature terminations is the same as in the coaxial case above, and the uncertainties in the output noise temperatures and the nonambient input noise temperature are treated in the next subsection. Reflection coefficients and S-parameters measured at on-wafer reference planes have larger uncertainties than those measured at reference planes in coaxial lines. The input uncertainties that we use for the on-wafer reflection coefficients and S-parameters (other than $|S_{21}|$) are $u_{\rm unc} = 0.004$ and $u_{\rm cor} = 0.003$, which correspond to $u(\Gamma) = 0.005$ and $\rho = 0.36$. For on-wafer measurements, we currently use the same uncertainties for large and small $|\Gamma|$.

B. Uncertainties in On-Wafer Noise Temperatures

The noise temperature at plane 2 (i.e., $T_{2,i}$) is given in terms of the measured noise temperature at plane $2'$ (i.e., $T_{2',i}$) by

$$T_{2,i} = \frac{T_{2',i} - (1-\alpha_{2'2,i})T_a}{\alpha_{2'2,i}} \tag{11}$$

where $\alpha_{2'2,i}$ is the available power ratio from plane 2 to plane $2'$ for termination i, and T_a is the noise temperature of the probe, which is assumed to be at ambient temperature. The available power ratio is given by

$$\alpha_{2'2,i} = \frac{|S_{2'2}|^2\left(1-|\Gamma_{2,i}|^2\right)}{|1-\Gamma_{2,i}S_{22}|^2\left(1-|\Gamma_{2',i}|^2\right)} \tag{12}$$

where $S_{2'2}$ is the S-parameter of probe 2 from plane $2'$ to plane 2, S_{22} is the reflection S-parameter of probe 2 at plane 2 (what would normally be called S_{11}), $\Gamma_{2,i}$ is the reflection coefficient at plane 2 (from the transistor), and $\Gamma_{2',i}$ is the reflection coefficient at plane $2'$ (from the probe).

From (11), we can see that to compute the uncertainty in the on-wafer output noise temperature $T_{2,i}$, we need the uncertainties in T_a, $T_{2',i}$, and $\alpha_{2'2,i}$. The uncertainty in T_a is the same as in the case of the previously treated coaxial amplifier measurements. The probe effect, of course, was absent from the treatment of the preceding section, and there is also a new complication for the noise measurement at the coaxial plane $T_{2',i}$. Because the on-wafer transistor may have a relatively large value of $|S_{22}|$, the reflection coefficient at the coaxial measurement plane $\Gamma_{2',i}$ can also be large. For values of $|\Gamma_{2',i}|$ that are larger than about 0.2, the uncertainty in $T_{2',i}$ increases, and the approximation of (10) is no longer adequate. This occurs because as $|\Gamma_{2',i}|$ increases, the mismatch correction increases, and a larger mismatch correction magnifies any error in the measurement of the reflection coefficient. An examination of the radiometer equation for NIST's NFRad system [10] reveals that $(T_{2',i} - T_a) \propto (1 - |\Gamma_{2',i}|^2)^{-1}$. Because (12) indicates that $\alpha_{2'2,i} \propto (1 - |\Gamma_{2',i}|^2)^{-1}$ as well, we can effect some simplification by regrouping (11) as

$$T_{2,i} = \frac{1}{\alpha'} T'_{2',i} + T_a \tag{13}$$

where we have suppressed the subscripts on α for convenience and pulled out and cancelled factors of $(1 - |\Gamma_{2',i}|^2)$ by defining $\alpha' \equiv (1-|\Gamma_{2',i}|^2)\alpha$ and $T'_{2',i} \equiv (1-|\Gamma_{2',i}|^2) \times (T_{2',i} - T_a)$. The advantages of the form in (13) are that it removes the necessity of dealing with important correlations between the errors in α and $T_{2',i}$ and that we can use (10) for the uncertainty in $T'_{2',i}$. From the usual rules for the propagation of uncertainty [5], the uncertainty in $T_{2,i}$ can be written as

$$u^2(T_{2,i}) = \frac{1}{\alpha'^2} u^2\left(T'_{2',i}\right) + \frac{(T_{2,i} - T_a)^2}{\alpha'^2} u^2(\alpha') + u^2(T_a) \tag{14}$$

where we have used $T'_{2',i}/\alpha' = T_{2,i} - T_a$ in the second term on the right side.

As already mentioned, $u(T'_{2'}, i)$ and $u(T_a)$ can be treated as in the coaxial amplifier case above. For α', we use its definition and (12), along with the propagation of uncertainty, to write

$$u^2(\alpha') \approx \left(\frac{2\alpha'}{|S_{2'2}|}\right)^2 u^2\left(|S_{2'2}|\right) + \left(\frac{2\alpha'|\Gamma_{2,i}|}{1 - |\Gamma_{2,i}|^2}\right)^2 u^2\left(|\Gamma_{2,i}|\right) \tag{15}$$

where a small term has been discarded. The uncertainty for on-wafer reflection-coefficient measurements was discussed in the preceding subsection. The relevant numbers for use in (15) are $u(|S_{2'2}|) = u(|\Gamma_{2,i}|) = 0.005$.

V. Physical Bounds and "Bad" Results

Basic physics and mathematics place certain constraints on the noise parameters. Some of the constraints are obvious in either the IEEE representation or the X representation. For example, $T_{\min}$, t, X_1, and X_2 must all be positive, and $2|X_{12}| \leq X_1 + X_2$. Some are less obvious, such as $|\eta| \geq 2$, where η is a function that arises in the transformation from the X-parameters to IEEE parameters, and is defined by

$$\eta = \frac{X_2\left(1 + |S_{11}|^2\right) + X_1 - 2\mathrm{Re}\left(S_{11}^* X_{12}\right)}{(X_2 S_{11} - X_{12})}. \tag{16}$$

That $|\eta| \geq 2$ can be proved by using (2) to write the numerator and denominator of (16) in terms of the c wave amplitudes. The numerator can be put in the form

$$X_2\left(1 + |S_{11}|^2\right) + X_1 - 2\mathrm{Re}\left(S_{11}^* X_{12}\right) = \left\langle \left|\left(\frac{c_2}{S_{21}}\right)^*\right|^2 + \left|\frac{c_2 S_{11}}{S_{21}} - c_1\right|^2 \right\rangle \tag{17}$$

whereas the denominator is given by

$$X_2 S_{11} - X_{12} = \left(\frac{c_2}{S_{21}}\right)^* \left(\frac{c_2 S_{11}}{S_{21}} - c_1\right). \tag{18}$$

That $|\eta| \geq 2$ then follows from the Schwarz inequality. For the noise parameters of poorly matched transistors, this is one of the most commonly violated bounds.

In actual measurements, as well as in the simulations of the MC program discussed below, it is possible to obtain unphysical results that violate these bounds. This is rare when measuring well-matched amplifiers, but it is not uncommon when measuring poorly matched very low-noise transistors on a wafer. Small measurement errors can conspire to yield fitted results for the noise parameters that are slightly (or even dramatically) outside the physical bound rather than slightly within it. One approach to this problem would be to constrain the fitting procedure so that the fitting parameters range only over physically allowed values. Instead, we choose to perform an unconstrained fit and to test whether the result satisfies the physical bounds. If any physical bound is violated, then that set of simulated measurements is discarded, as would a set of real measurements that violated physical bounds. This has the advantage of alerting us when the measurement results prefer an unphysical solution for the noise parameters, rather than just finding the best physical solution. (It is also considerably easier than imposing this set of constraints in the fit.)

We impose two further cuts on the set of simulated results. If the best fit is not good enough, we discard that set of simulated measurements, as we would with a set of real measurements that did not admit a good enough fit. For this purpose, we define "good enough" by $\chi^2/\nu \leq 1$, where ν is the number of degrees of freedom in the fit. In several instances, we have also evaluated the uncertainties with a cut of $\chi^2/\nu \leq 1.5$, and it makes little difference. The other cut is on the uncertainty in Γ_{opt}. It sometimes happens that an acceptable fit is obtained, but that the variance of Γ_{opt} is enormous (corresponding to an extremely flat minimum in this variable). A real measurement set with this property would be discarded, and we do so in the simulation as well. The maximum standard deviation allowed for either the real or imaginary part of Γ_{opt} is 1.

VI. Results and Conclusion

A. Sample Results

The preceding analysis was used for the measurements of the noise parameters of an on-wafer transistor fabricated in 0.13-μm CMOS technology [2]. The set of input terminations for the forward configuration comprised one hot source (around 1100 K) and eight ambient-temperature terminations (296.15 K). One reverse measurement was also made with a matched ambient-temperature load connected at plane $1'$. In the forward measurements, a 10-dB attenuator was connected between probe 2 and the radiometer to keep the measured noise within the linear range of the radiometer. The results for the X-parameters are reproduced in Fig. 3. The

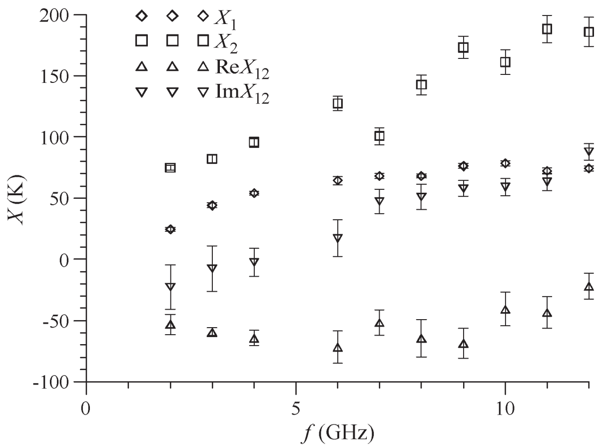

Fig. 3. Results and uncertainties for the X-parameters of a transistor on a wafer.

corresponding graphs for the IEEE noise parameters can be found in [2] or [4]. The approximate values for the uncertainties in the IEEE on-wafer noise parameters are 0.22–0.30 dB for G_0, 0.2–0.3 dB for $F_{\min}$, 15–25 K for $T_{\min}$, 0.6–0.8 Ω for R_n, 0.02–0.07 for $|\Gamma_{\rm opt}|$, and 1° to 6° for $\phi_{\rm opt}$. The uncertainties in the on-wafer case are generally somewhat larger than for a connectorized amplifier. In both cases, the uncertainties are overestimated due to the treatment of the output attenuator. In [2] and [4] and therefore in Fig. 3, correlations in the errors due to the attenuator, for different terminations, were not included. These correlations are now incorporated in the program and are reflected in the results presented in [13].

B. Conclusion

We have set forth an uncertainty analysis for the NIST measurements of the noise parameters of amplifiers and transistors, where the reference planes can be either in coaxial transmission lines or on a wafer. The standard uncertainty is the root sum of the squares of the type A and type B uncertainties. The type A uncertainties are determined in the weighted least-square fit to the overdetermined system of equations that result from the measurements of the output noise temperatures for different configurations and terminations. The type B uncertainties are evaluated by an MC procedure. The uncertainty analysis described has been used for both coaxial low-noise amplifiers [1], [13] and very poorly matched on-wafer CMOS transistors [2]. In the amplifier case [1], the results were subjected to checks and verification that confirmed the general validity of the uncertainties, as well as the actual values of the parameters.

Acknowledgment

The author thanks D. Walker of NIST for many discussions and for performing the measurements to which this analysis is applicable. He also thanks K. Wong of Agilent for requesting this paper.

References

[1] J. Randa and D. K. Walker, “Amplifier noise-parameter measurement checks and verification,” in *63rd ARFTG Conf. Dig.*, 2004, pp. 41–45.
[2] J. Randa and D. K. Walker, “On-wafer measurement of transistor noise parameters at NIST,” *IEEE Trans. Instrum. Meas.*, vol. 56, no. 2, pp. 551–554, Apr. 2007.
[3] J. Randa, “Uncertainty analysis for noise-parameter measurements,” in *CPEM Conf. Dig.*, 2008, pp. 498–499.
[4] J. Randa, *Uncertainty Analysis for NIST Noise-Parameter Measurements.* Boulder, CO: NIST, Mar. 2008. NIST Tech. Note 1530. [Online]. Available: http://boulder.nist.gov/div818/81801/Noise/publications/
[5] J. Randa, “Noise-parameter uncertainties: A Monte Carlo simulation,” *J. Res. Nat. Inst. Stand. Technol.*, vol. 107, no. 5, pp. 431–444, 2002.
[6] S. Wedge and D. Rutledge, “Wave techniques for noise modeling and measurement,” *IEEE Trans. Microw. Theory Tech.*, vol. 40, no. 11, pp. 2004–2012, Nov. 1992.
[7] H. Haus *et al.*, “IRE standards on methods of measuring noise in linear twoports, 1959,” *Proc. IRE*, vol. 48, no. 1, pp. 60–68, Jan. 1960.
[8] W. H. Press, B. P. Flannery, S. A. Teukolsky, and W. T. Vetterling, *Numerical Recipes*. Cambridge, U.K.: Cambridge Univ. Press, 1986, ch. 14.5.
[9] J. Randa, *Uncertainty in NIST Noise-Temperature Measurements.* Boulder, CO: NIST, Mar. 1998. NIST Tech. Note 1502. [Online]. Available: http://boulder.nist.gov/div818/81801/Noise/publications/
[10] C. A. Grosvenor, J. Randa, and R. L. Billinger, *Design and Testing of NFRAD—A New Noise Measurement System.* Boulder, CO: NIST, Mar. 2000. NIST Tech. Note 1518. [Online]. Available:http://boulder.nist.gov/div818/81801/Noise/publications/
[11] R. Marks, “A multiline method of network analyzer calibration,” *IEEE Trans. Microw. Theory Tech.*, vol. 39, no. 7, pp. 1205–1215, Jul. 1991.
[12] D. Williams and R. Marks, “Transmission line capacitance measurement,” *IEEE Microw. Guided Wave Lett.*, vol. 1, no. 9, pp. 243–245, Sep. 1991.
[13] D. Gu, D. K. Walker, and J. Randa, “Noise-parameter measurement with automated variable terminations,” *IEEE Trans. Instrum. Meas*. to be published.

James Randa (M’84–SM’91) received the Ph.D. degree in physics from the University of Illinois at Urbana-Champaign in 1974.

He then held Postdoctoral and/or faculty positions with Texas A&M University, College Station; the University of Manchester, Manchester, U.K.; and the University of Colorado at Boulder. During this time, he did research on the phenomenology of elementary particles and on theories of fundamental interactions. Since 1983, he has been with the Electromagnetics Division, National Institute of Standards and Technology (NIST), Boulder. From 1983 to 1994, he was with the Fields and Interference Metrology Group, NIST, where he worked on various topics in electromagnetic interference metrology. From 1994 to 2008, he was with the RF Electronics Group, NIST, where he worked on thermal noise metrology. He retired from NIST in 2008 and is currently a Guest Researcher with NIST and a Senior Research Associate with the Physics Department, University of Colorado at Boulder.

Dr. Randa has chaired the High-Frequency Working Group (GT-RF) of the Consultative Committee on Electricity and Magnetism (CCEM) since 2002.